Hindawi Publishing Corporation
Mobile Information Systems
Volume 2016, Article ID 2152538, 11 pages
http://dx.doi.org/10.1155/2016/2152538

Research Article

Rank-Constrained Beamforming for MIMO Cognitive Interference Channel

Duoying Zhang, Yao Zhang, Zujian Wu, and Huiqin Du

College of Information Science and Technology, Jinan University, Guangzhou 510632, China

Correspondence should be addressed to Huiqin Du; duhq518@gmail.com

Received 29 January 2016; Revised 14 April 2016; Accepted 5 May 2016

Academic Editor: Yunfei Chen

This paper considers the spectrum sharing multiple-input multiple-output (MIMO) cognitive interference channel, in which multiple primary users (PUs) coexist with multiple secondary users (SUs). Interference alignment (IA) approach is introduced that guarantees that secondary users access the licensed spectrum without causing harmful interference to the PUs. A rank-constrained beamforming design is proposed where the rank of the interferences and the desired signals is concerned. The standard interferences metric for the primary link, that is, *interference temperature*, is investigated and redesigned. The work provides a further improvement that optimizes the dimension of the interferences in the cognitive interference channel, instead of the power of the interference leakage. Due to the nonconvexity of the rank, the developed optimization problems are further approximated as convex form and are solved via choosing the transmitter precoder and receiver subspace iteratively. Numerical results show that the proposed designs can improve the achievable degree of freedom (DoF) of the primary links and provide the considerable sum rate for both secondary and primary transmissions under the rank constraints.

1. Introduction

Cognitive radio (CR) network is a potential solution to enhance spectrum utilization by allowing coexistence with licensed networks. The concurrent transmissions are allowed in the spectrum sharing cognitive radio networks by keeping the CR interferences to the primary user receivers (PU-Rxs) under an acceptable level. Hence, an effective approach to control the interference level is of critical importance to underlay CR networks.

Recently, interference alignment (IA) has been developed to achieve the maximum spatial degrees of freedom in the K user interference channel, which guarantees an interference-free received signal by forcing interferences into a reduced-dimensional receiver subspace [1–13]. Considering its potential to mitigate the interference, the IA is widely introduced to multiple-input multiple-output (MIMO) cognitive radio system [14–19], MIMO relay system [20], multihop MIMO networks [21], and the simultaneous wireless information and power transfer (SWIPT) system [22]. In the MIMO CR networks, the upper bound and lower bound of achievable degrees of freedom (DoF) have been studied with global channel information [1, 23], and the CR interferences to the PUs are nulled in [14–16]. However, the global channel state information usually is not available, which may lead to severe CR interferences to PU. As a result, the practical algorithm is developed that minimizes the interference leakage power by selecting the precoding and receiving beamforming matrices alternatively [16, 23–25]. In [16], the active IA and success interference cancelation (SIC) techniques are combined to transmit data over MIMO underlay CR network. Moreover, an efficient antenna selection IA algorithm based on discrete stochastic optimization (DSO) is proposed to improve the received signal-to-interference-and-noise ratio (SINR) of each user in IA-based CR networks with low complexity [17]. In the abovementioned works, the interference temperature is considered as a standard interference *metric* that suppresses the CR interferences and guarantees the quality of service (QoS) of the primary transmission. Considering the available eigenmodes distributed among the SUs and PUs, the adaptive number of eigenmodes beamforming (ANEB) algorithm for the PU is developed which adjusts the number of PU's eigenmodes to meet its rate requirement [26]. It suggests that the DoF of the receiving eigenspace is of crucial

importance to the system performance, which motivates us to revise the standard interference *metric*, that is, interference temperature, in the underlay CR networks.

In this paper, the rank-constrained beamforming design is developed for underlay MIMO CR network. Instead of using the standard interference metric, *interference temperature*, the CR interferences to the PU-Rxs are controlled by a rank constraint that aligns the CR interferences into a reduced-dimensional subspace. As a result, the CR interferences are suppressed in a low-dimensional subspace, rather than an acceptable low level of the received power; consequently the achievable DoF of the intended primary signal is guaranteed. The optimal transmit precoding and receiving beamforming are selected by minimizing the total interference of the secondary transmission subject to the rank constraint on the CR interferences. Different from those designs based on Cadambe-Jafar scheme [14–16], the proposed design strives to null the CR interferences at the PU-Rxs without the global channel state information. Considering the benefits of the multiplexing gain/DoF, we further maximize the achievable DoF of the secondary links by minimizing the dimension of the interferences of the secondary transmission while maintaining the full rank of the desired signal matrix and the low rank of the CR interferences to PUs. Due to the nonconvexity of the rank, the proposed optimization problem can be approximated as convex form and efficiently solved via alternating minimization. Simulation results show that the proposed scheme can improve the sum rate of both PU and SUs due to the effective rank constraint on the CR interferences.

This paper is organized as follows. The system model is introduced in Section 2. Section 3 presents the rank-constrained interference minimization algorithm, followed by further improvement in Section 4. Simulation results are presented and discussed in Section 5. Concluding remarks are given in Section 6.

Notations. Matrices and vectors are type-faced using slanted bold uppercase and lowercase letters, respectively. Conjugate transpose of the matrix $\mathbf{A}$ is denoted as $\mathbf{A}^H$. Positive semidefiniteness of the matrix $\mathbf{A}$ is depicted using $\mathbf{A} \succeq 0$, and $\mathbf{I}_d$ is an identity matrix with the dimension equal to d. $\mathbb{C}^{m\times n}$ is used to describe the complex space of $m \times n$ matrices, and $\mathcal{CN}(\mathbf{m}, \mathbf{\Sigma})$ denotes a complex Gaussian distribution with mean $\mathbf{m}$ and covariance $\mathbf{\Sigma}$. Finally, mathematical expectation is described as $\mathsf{E}[\cdot]$. The trace, nuclear norm, and Frobenius norm of a matrix/vector are denoted by $\mathrm{tr}\{\cdot\}$, $\|\cdot\|_*$, and $\|\cdot\|_F$, respectively.

2. System Model

Consider a MIMO cognitive radio network with L PU and K SUs, shown in Figure 1. The secondary transmitter (SU-Tx) is equipped with N_k transmit antennas and M_k receiving antennas at the kth SU. The transmission of all K users is synchronized such that each simultaneously begins and ends each transmission, and no frequency or timing offsets exist in the network [2, 6]. In the primary links, there are N_p transmit antennas and M_p receiving antennas equipped at each PU.

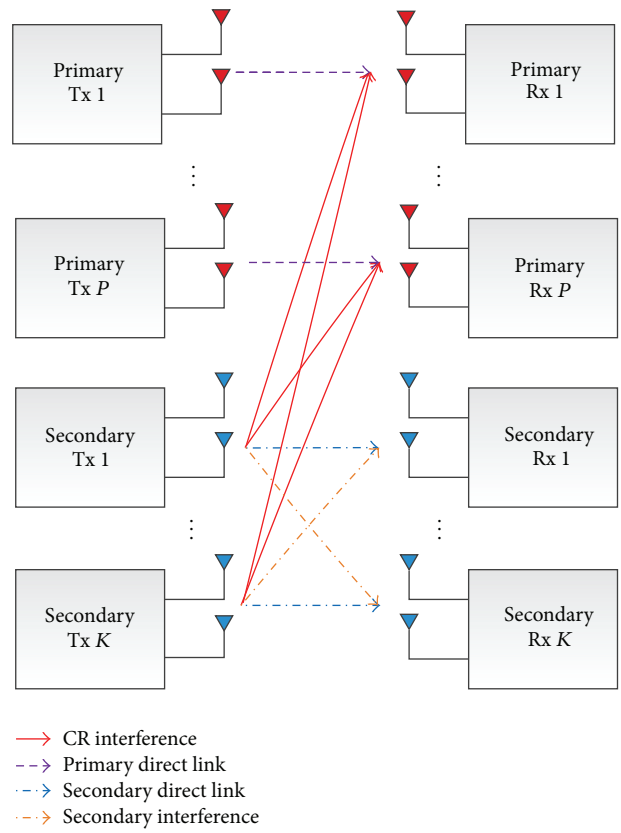

Figure 1: MIMO underlay cognitive radio network with single primary link and K secondary pairs.

Without any loss of generality, we assume that the users are indexed so that users $1, \ldots, K$ are SUs and the users $1, \ldots, L$ are the PUs. The total signal received at the kth secondary user receiver (SU-Rx) can be expressed as

$$\mathbf{y}_k = \mathbf{H}_{kk}\mathbf{V}_k\mathbf{x}_k + \sum_{l=1, l\neq k}^{K} \mathbf{H}_{kl}\mathbf{V}_l\mathbf{x}_l + \mathbf{n}_k, \quad k = 1, \ldots, K, \tag{1}$$

where $\mathbf{x}_k \in \mathbb{C}^{d_k\times 1}$ represents the transmitted signal from the kth SU-Tx with equally loaded power and $\mathbf{H}_{kl} \in \mathbb{C}^{M_k\times N_k}$ denote the flat-fading channel from the lth SU-Tx to the kth SU-Rx receiver. The columns of the precoding matrix $\mathbf{V}_k \in \mathbb{C}^{N_k\times d_k}$ are orthonormal basis of the kth transmitted signal where $\mathbf{V}_k^H\mathbf{V}_k = \mathbf{I}$ (for all k), and the receiver thermal noise $\mathbf{n}_k \in \mathbb{C}^{N_k\times 1}$ is assumed as the complex additive white Gaussian noise with covariance $\sigma_k^2\mathbf{I}$; that is, $\mathbf{n}_k \sim \mathcal{CN}(\mathbf{0}, \sigma_k^2\mathbf{I})$. Note that any interference from the PU-Tx is assumed to be neglected. (This can be possible if the PU-Tx is located far away from the secondary users, or the interference is represented by the noise under an assumption that the PU-Tx's signal is generated by random Gaussian codebooks [27]. In IEEE 802:22 standard, the secondary wireless regional area network (WRAN) is located far away from the primary TV transmitter and hence the interference from the primary TV

transmitter can be neglected at the receiver.) Similarly, the received signal $\mathbf{y}_p$ at the pth PU-Rx can be expressed as

$$\mathbf{y}_p = \mathbf{H}_{pp}\mathbf{V}_p\mathbf{x}_p + \sum_{p=1,p\neq q}^{L}\mathbf{H}_{pq}\mathbf{V}_q\mathbf{x}_q + \sum_{k=1}^{K}\mathbf{H}_{pk}\mathbf{V}_k\mathbf{x}_k + \mathbf{n}_p, \quad p = 1,\ldots,L, \tag{2}$$

where $\mathbf{x}_p \in \mathbb{C}^{d_p\times 1}$ represents the transmitted signal from the pth PU-Tx with equally loaded power, $\mathbf{H}_{pq} \in \mathbb{C}^{M_p\times N_p}$ denote the channel from the qth PU-Tx to the pth PU-Rx, and $\mathbf{H}_{pk} \in \mathbb{C}^{M_p\times N_k}$ is the channel from the kth SU-Tx to the pth PU-Rx. The columns of the precoding matrix $\mathbf{V}_p \in \mathbb{C}^{N_p\times d_p}$ are orthonormal basis of the transmitted signal from the pth PU-Tx, and the receiver thermal noise $\mathbf{n}_p \in \mathbb{C}^{N_p\times 1}$ is assumed as the complex additive white Gaussian noise with covariance $\sigma_p^2\mathbf{I}$; that is, $\mathbf{n}_p \sim \mathcal{CN}(\mathbf{0},\sigma_p^2\mathbf{I})$. Note that the first term in (2) is the received intended signal of the pth primary link, the second term is the interferences from other primary links, and the third term is the CR interferences to the corresponding PU-Rx.

In the underlay CR network, the secondary base stations are allowed to concurrently transmit data as long as the interference metric has been satisfied. Previous researches nulled the CR interferences at the PU-Rxs with global channel state information, in which the CR interferences can be completely aligned in the receiver subspace of the primary user [14–16]. However, the global channel state information is usually not available in practice, in which the CR interferences at the PU-Rxs may be difficultly eliminated, leading to the performance degradation of the primary links. Without the global channel state information, the well-known interference *metric* that is used to control the CR interferences is named as interference temperature; that is,

$$\mathbf{IT}_{pk} = \left\|\mathbf{U}_p^H\mathbf{H}_{pk}\mathbf{V}_k\right\|_F, \tag{3}$$

where $\mathbf{U}_p \in \mathbb{C}^{M_p\times d_p}$ is the receiver beamforming matrix of the pth PU. Note that the interference temperature is used to suppress the CR interferences under an acceptable power level, rather than a reduced-dimensional subspace. However, the standard IA techniques suggest that the interference-free subspace can provide high DoF of the desired signal and provide considerable average sum rate at that moderate and high signal-to-noise ratio (SNR) [28, 29], which motivates us to further investigate another interference *metric* that can provide more dimensions of the interference-free receiver subspace.

3. Rank-Constrained Interference Minimization Beamforming

The CR interference *metric* is of critical importance to the secondary transmission in the underlay CR network. It works as admission control; that is, the secondary transmission is allowed once the QoS of the primary links is satisfied; otherwise, it will be prohibited to transmit. The ideal scenario is that the CR interference is completely aligned and that there are no CR interferences to each PU-Rx, as suggested in [14–16]. With respect to the dimension of the receiver subspace, the ideal scenario that CR interference is canceled can be expressed in the following equation; that is,

$$\operatorname{rank}\left(\mathbf{J}_p\right) = \operatorname{rank}\left(\mathbf{U}_p^H\left\{\mathbf{H}_{pk}\mathbf{V}_k\right\}_{k=1}^{K}\right) = 0, \tag{4}$$

where $\mathbf{J}_p$ is defined as the CR interferences to the pth PU-Rx; that is, $\mathbf{J}_p = \mathbf{U}_p^H[\mathbf{H}_{p1}\mathbf{V}_1,\ldots,\mathbf{H}_{pk}\mathbf{V}_k,\ldots,\mathbf{H}_{pK}\mathbf{V}_K]$. Supposing that the interferences coming from other primary links are perfectly aligned, the achievable multiplexing gain per PU can be expressed as

$$\mathrm{DoF}_p = \left[\operatorname{rank}\left(\mathbf{U}_p^H\mathbf{H}_{pp}\mathbf{V}_p\right) - \operatorname{rank}\left(\mathbf{J}_p\right)\right]^+, \tag{5}$$

where $\operatorname{rank}(\mathbf{U}_p^H\mathbf{H}_{pp}\mathbf{V}_p) \geq \operatorname{rank}(\mathbf{J}_p)$, or else $\mathrm{DoF}_p = 0$. To minimize the DoF degradation of the pth primary link caused by the CR interferences, the effective approach is to force the CR interferences from the SU-Txs to share a reduced-dimensional subspace at the PU-Rxs, leading to an interference-free receiver subspace for the primary transmission.

Without global channel state information (in this work, the local channel information is followed by the definition in [6], where each of the transmitters is assumed to know only the channel to its desired transmitter and the covariance matrix of its effective noise (consisting of the AWGN and the interference from all other users), e.g., the local channel information of the kth link including the direct channel $\mathbf{H}_{kk}$ and desired link $\{\mathbf{H}_{lk}\}_{l=1,l\neq k}^{K}$, while the global channel information is defined as that in [1] where each node has to know all the channels $\{\{\mathbf{H}_{lk}\}_{l=1}^{K}\}_{k=1}^{K}$), each secondary link primarily can adjust its precoding and receiver subspaces to minimize the interference leaked to unintended SU-Rxs. More specifically, the precoder matrices $\{\mathbf{V}_l\}_{l=1}^{K}$ and interference receiving matrices $\{\mathbf{U}_k\}_{k=1}^{K}$ are chosen such that each SU-Rx can decode its own signal by minimizing the interference leakage while forcing the CR interferences to share a reduced-dimensional subspace at the PU-Rxs. The underlying optimization problem can be mathematically described as follows:

$$\underset{\mathbf{U}_k,\mathbf{V}_l}{\text{minimize}} \quad \sum_{k=1}^{K}\sum_{l=1,l\neq k}^{K}\left\|\mathbf{U}_k^H\mathbf{H}_{kl}\mathbf{V}_l\right\|_F^2, \tag{6}$$

$$\text{subject to} \quad \operatorname{rank}\left(\mathbf{J}_p\right) = 0, \tag{7}$$

$$\operatorname{rank}\left(\mathbf{U}_k^H\mathbf{H}_{kk}\mathbf{V}_k\right) = d_k, \tag{8}$$

where $\mathbf{U}_k \in \mathbb{C}^{M\times d_k}$ presents the receiving beamforming matrix whose columns are the orthonormal basis of the kth SU receiver. The objective function (6) minimizes the total interference leakage of the secondary transmission, and the full rank of the desired signals of the secondary links is guaranteed in (8). However, the rank constraints in (7) and (8) are not convex, and possible approximations are required.

In order to minimize the performance degradation from the secondary links, it is reasonable to approximate the rank constraint (7) as a nuclear norm with a prespecified small value ε; that is,

$$\left\|\mathbf{J}_p\right\|_* \leq \varepsilon, \tag{9}$$

which can align the CR interferences into a low-dimensional subspace, where $\|\mathbf{A}\|_*$ is denoted as nuclear norm of the matrix $\mathbf{A}$. Such approximation has been well studied in compressive sensing and sparse matrix completion problems, such as [30, 31] and references therein. Moreover, the rank constraint (9) on the desired signal can be replaced by Hermitian positive semidefinite matrix; that is,

$$\sigma_{\min}\left(\mathbf{U}_k^H\mathbf{H}_{kk}\mathbf{V}_k\right) \geq \epsilon, \quad \mathbf{U}_k^H\mathbf{H}_{kk}\mathbf{V}_k \succeq 0, \tag{10}$$

where $\sigma_{\min}(\mathbf{A})$ denotes the minimum singular value of the matrix $\mathbf{A}$. Note that the closed set, $\sigma_{\min}(\mathbf{U}_k^H\mathbf{H}_{kk}\mathbf{V}_k) \geq \epsilon$ and $(\mathbf{U}_k^H\mathbf{H}_{kk}\mathbf{V}_k) \succeq 0$, is a subset of Hermitian positive definite matrix; that is, $\mathbf{U}_k^H\mathbf{H}_{kk}\mathbf{V}_k = (\mathbf{U}_k^H\mathbf{H}_{kk}\mathbf{V}_k)^H$ and $\sigma_{\min}(\mathbf{U}_k^H\mathbf{H}_{kk}\mathbf{V}_k) > 0$. As ϵ gets closer to 0, the two sets asymptotically overlap [28]. As a result, the underlying rank-constrained problem can be approximated as

$$\underset{\mathbf{U}_k,\mathbf{V}_l}{\text{minimize}} \quad \sum_{k=1}^{K}\sum_{l=1,l\neq k}^{K}\left\|\mathbf{U}_k^H\mathbf{H}_{kl}\mathbf{V}_l\right\|_F^2, \tag{11}$$

$$\text{subject to} \quad \left\|\mathbf{J}_p\right\|_* \leq \varepsilon, \tag{12}$$

$$\sigma_{\min}\left(\mathbf{U}_k^H\mathbf{H}_{kk}\mathbf{V}_k\right) \geq \epsilon, \quad \mathbf{U}_k^H\mathbf{H}_{kk}\mathbf{V}_k \succeq 0. \tag{13}$$

The remaining problem is still nonconvex due to simultaneously optimizing the precoding matrix $\mathbf{V}_k$ and the receiving beamforming matrix $\mathbf{U}_k$; therefore, the alternating minimization is introduced; that is, temporarily holding the receiver matrices fixed, we can optimize the objective function for the remaining variables, alternating between which variables are held fixed and which are updated. More specifically, with fixed $\{\mathbf{U}_l\}_{l=1}^K$, the precoders $\{\mathbf{V}_k\}_{k=1}^K$ are obtained by solving the following problem:

$$\begin{aligned}
&\underset{\mathbf{V}_k}{\text{minimize}} \quad \sum_{k=1}^{K}\sum_{l=1,l\neq k}^{K}\left\|\mathbf{U}_l^H\mathbf{H}_{lk}\mathbf{V}_k\right\|_F^2,\\
&\text{subject to} \quad \sum_{k=1}^{K}\left\|\mathbf{U}_p^H\mathbf{H}_{pk}\mathbf{V}_k\right\|_* \leq \varepsilon,\\
&\qquad\qquad \sigma_{\min}\left(\mathbf{U}_k^H\mathbf{H}_{kk}\mathbf{V}_k\right) \geq \epsilon, \quad \mathbf{U}_k^H\mathbf{H}_{kk}\mathbf{V}_k \succeq 0.
\end{aligned} \tag{14}$$

Then, the receiver matrices $\{\mathbf{U}_k\}_{k=1}^K$ are achieved by using the solutions $\{\mathbf{V}_l\}_{l=1}^K$ as an input, such as

$$\begin{aligned}
&\underset{\mathbf{U}_k}{\text{minimize}} \quad \sum_{k=1}^{K}\sum_{l=1,l\neq k}^{K}\left\|\mathbf{U}_k^H\mathbf{H}_{kl}\mathbf{V}_l\right\|_F^2,\\
&\text{subject to} \quad \sigma_{\min}\left(\mathbf{U}_k^H\mathbf{H}_{kk}\mathbf{V}_k\right) \geq \epsilon, \quad \mathbf{U}_k^H\mathbf{H}_{kk}\mathbf{V}_k \succeq 0.
\end{aligned} \tag{15}$$

Given: $\varepsilon \geq 0$, and $\epsilon \geq 0$, $\mathbf{U}_0$, and $\mathbf{U}_k^{(0)}$
repeat
(1) Solve the subproblem (14) with fixed $\mathbf{U}_k^{(i-1)}$,
Output $\mathbf{V}_k^i$
(2) Solve the subproblem (15) with fixed $\mathbf{V}_k^{(i)}$,
Output $\mathbf{U}_k^i$
until objective function $\|\text{Obj}^{(i)} - \text{Obj}^{(i-1)}\| \leq \varsigma$
Output: $\mathbf{U}_k^{\text{opt}}$, and $\mathbf{V}_k^{\text{opt}}$

Algorithm 1: Rank-constrained beamforming design.

Now, each optimization problem is convex which can be solved by using CVX toolbox [32]. We continue by iterating this process until it converges in terms of the cost function or stop it when the iteration number achieves the maximum prespecified number. Note that the constraint on the CR interferences to the PU is not included when selecting the receiving beamforming. The step-by-step algorithm is presented in Algorithm 1.

Proposition 1. *Under the same prespecified interference threshold, the nuclear norm constraint (12) is equal to or tighter than the interference temperature constraint (3) in terms of power.*

Proof. Supposing the matrix $\mathbf{A} \in \mathbb{C}^{m\times n}$ with rank r, the matrix norm inequality is held [33]; that is,

$$\|\mathbf{A}\|_F \leq \|\mathbf{A}\|_*, \tag{16}$$

where the Frobenius norm $\|\mathbf{A}\|_F = \sqrt{\text{tr}\{\mathbf{A}^H\mathbf{A}\}} = \sqrt{\sum_{i=1}^{\min\{m,n\}}\sigma_i^2}$ and the nuclear norm $\|\mathbf{A}\|_* = \text{tr}\{\sqrt{\mathbf{A}^H\mathbf{A}}\} = \sum_{i=1}^{\min\{m,n\}}\sigma_i$ (σ_i is the ith singular value of the matrix $\mathbf{A}$). Once the optimum solution is achieved, we have

$$\begin{aligned}
&\left\|\mathbf{U}_p^H\mathbf{H}_{pk}\mathbf{V}_k^{*\text{IM}}\right\|_F = \varepsilon,\\
&\left\|\mathbf{U}_p^H\mathbf{H}_{pk}\mathbf{V}_k^{*\text{RCIM}}\right\|_F \leq \left\|\mathbf{U}_p^H\mathbf{H}_{pk}\mathbf{V}_k^{*\text{RCIM}}\right\|_* = \varepsilon,
\end{aligned} \tag{17}$$

under the same prespecified interference threshold, where $\mathbf{V}_k^{*\text{IM}}$ is defined as the optimal precoding under the standard interference temperature and $\mathbf{V}_k^{*\text{RCIM}}$ is the optimal precoding under the nuclear norm constraint. It leads to the result straightforwardly obtained. □

Remark 1. Since the nuclear norm is a surrogate approximation of the rank, the optimization problem under the rank constraint (7) leaks fewer CR interferences to the PU-Rx in terms of power, compared with that under the standard interference temperature.

Remark 2. It is worth emphasizing the key difference between the optimization problem with the proposed rank constraint and that with standard interference temperature [16, 17, 23–25]. Although it seems simple to replace the rank constraint

on the CR interferences with the standard interference temperature, the proposed constraint actually provides a new way to investigate the interference *metric* of the CR network. Section 5 shows that the higher DoF of the primary links can be achieved under the new interference *metric* compared with that under the standard one.

Remark 3. Each iteration reduces the objective function $\sum_{k=1}^{K}\sum_{l=1,l\neq k}^{K}\|\mathbf{U}_k^H\mathbf{H}_{kl}\mathbf{V}_l\|_F^2$, which is the nonnegative function. As a result, it is clear that the objective function decreases monotonically. Moreover, the objective function is not jointly convex on $\mathbf{U}_k$ and $\mathbf{V}_k$. Hence, although each step of the proposed algorithms finds the minimum of the objective function over the optimized variables, the proposed algorithm is not guaranteed to converge to the global optimum; only local optimum is guaranteed. More details are presented in Section 5.

Remark 4. In this work, the precoders and receiving beamformers are iteratively optimized via the centralized approach which is difficult to implement for distributed SUs. Minimization of the interference subspace can be an alternative algorithm where the interference subspace of the kth SU can be expressed as $\mathbf{R}_k = [\mathbf{H}_{k1}\mathbf{V}_1,\ldots,\mathbf{H}_{k,k-1}\mathbf{V}_{k-1}, \mathbf{H}_{k,k+1}\mathbf{V}_{k+1},\ldots,\mathbf{H}_{kK}\mathbf{V}_K]$, and the optimization problem can be solved by following the process in [13].

4. Rank-Constrained Interference Rank Minimization Beamforming

Due to its effective interference elimination, the IA scheme has been introduced in CR network. Most recent works cancel the interferences of the secondary links in terms of power, such as interference leakage minimization [16, 23–25] and SINR maximization [17]. However, the key concept of the IA is to select precoder matrices $\{\mathbf{V}_k\}_{k=1}^K$ and receiver subspaces spanned by $\{\mathbf{U}_k\}_{k=1}^K$ such that each receiver can decode its own signal by forcing interfering users to share a reduced-dimensional subspace [1]

$$\begin{aligned}\operatorname{rank}\left(\mathbf{U}_k^H\mathbf{H}_{k,k}\mathbf{V}_k\right) &= d_k,\\ \mathbf{U}_k^H\mathbf{H}_{k,l}\mathbf{V}_l &= 0.\end{aligned} \tag{18}$$

In other words, the IA approach strives to maximize the achievable multiplexing gain per user. The interference-free subspace optimization framework can lead to better performance compared with the power optimizations, as suggested in [28, 29]. It motivates us to investigate the rank optimization framework in CR networks.

In order to understand the dimension optimization framework, we follow the definition of the *signal* and *interference* matrices of the secondary transmission [28, 29]:

$$\begin{aligned}&\mathbf{S}_k\left(\mathbf{U}_k,\mathbf{V}_k\right) \triangleq \mathbf{U}_k^H\mathbf{H}_{k,k}\mathbf{V}_k,\\ &\mathbf{J}_k\left(\mathbf{U}_k,\{\mathbf{V}_l\}_{l=1}^K\right)\\ &\quad\triangleq \mathbf{U}_k^H\left[\mathbf{H}_{k,1}\mathbf{V}_1,\ldots,\mathbf{H}_{k,l}\mathbf{V}_l,\ldots,\mathbf{H}_{k,K}\mathbf{V}_K\right],\end{aligned} \tag{19}$$

where the dimensions of signal and interference matrices are $\mathbf{S}_k \in \mathbb{C}^{d_k\times d_k}$ and $\mathbf{J}_k \in \mathbb{C}^{d_k\times[(K-1)d_k]}$. For simplicity, we refer to $\mathbf{S}_k(\mathbf{U}_k,\mathbf{V}_k)$ and $\mathbf{J}_k(\mathbf{U}_k,\{\mathbf{V}_l\}_{l=1}^K)$ as $\mathbf{S}_k$ and $\mathbf{J}_k$. Consequently, the achievable multiplexing gain of the kth SU can be expressed as

$$\mathrm{DoF}_k = \left[\operatorname{rank}\left(\mathbf{S}_k\right) - \operatorname{rank}\left(\mathbf{J}_k\right)\right]^+, \tag{20}$$

where $\operatorname{rank}(\mathbf{S}_k) \geq \operatorname{rank}(\mathbf{J}_k)$, or else $\mathrm{DoF}_k = 0$. To aim for d_k interference-free dimensions per SU, proper precoding and receiving beamforming matrices are selected to maximize the achievable DoF in (20) while maintaining the full rank of the desired signal of secondary user and aligning the CR interferences to a reduced-dimensional subspace of the primary receiver; that is,

$$\underset{\mathbf{V}_k,\{\mathbf{U}_k\}_{k=1}^K}{\text{minimize}} \quad \operatorname{rank}\left(\mathbf{J}_k\right), \tag{21}$$

$$\text{subject to} \quad \operatorname{rank}\left(\mathbf{S}_k\right) = d_k, \tag{22}$$

$$\operatorname{rank}\left(\mathbf{J}_p\right) = 0, \tag{23}$$

due to

$$\begin{aligned}&\underset{\mathbf{U}_k,\mathbf{V}_k}{\text{maximize}}\left[\operatorname{rank}\left(\mathbf{S}_k\right) - \operatorname{rank}\left(\mathbf{J}_k\right)\right]\\ &\quad\Longleftrightarrow \underset{\mathbf{U}_k,\mathbf{V}_k}{\text{maximize}}\left[d_k - \operatorname{rank}\left(\mathbf{J}_k\right)\right]\\ &\quad\Longleftrightarrow \underset{\mathbf{U}_k,\mathbf{V}_k}{\text{minimize}}\operatorname{rank}\left(\mathbf{J}_k\right).\end{aligned} \tag{24}$$

However, it is difficult to solve the K optimization problem in parallel, which can be reformulated as the sum of the interference dimension minimizations subject to the rank constraints instead. Moreover, the rank function is nonconvex and intractable, and hence, the underlying problem can be further approximated as

$$\begin{aligned}&\underset{\mathbf{V}_k,\{\mathbf{U}_k\}_{k=1}^K}{\text{minimize}} \quad \sum_{k=1}^{K}\left\|\mathbf{J}_k\right\|_*,\\ &\text{subject to} \quad \left\|\mathbf{J}_p\right\|_* \leq \varepsilon,\\ &\qquad\sigma_{\min}\left(\mathbf{U}_k^H\mathbf{H}_{kk}\mathbf{V}_k\right) \geq \epsilon, \quad \mathbf{U}_k^H\mathbf{H}_{kk}\mathbf{V}_k \succeq 0.\end{aligned} \tag{25}$$

The optimal precoding and receiving beamforming can be selected by alternating minimization algorithm, and the subproblems can be efficiently solved via CVX toolbox [34].

Remark 5. The objective function (21) can be approximated as the reweighted nuclear norm which uses the sum of log surrogate functions with a weight matrix. It can provide better approximation compared with the standard nuclear norm approximation, leading to an improvement of the sum rate and the achievable DoF, especially when the perfect IA is not feasible, suggested in [28]. In this work, we investigate the difference between the dimension optimization and the power optimization. Therefore, the further improvement of the objective function is beyond our discussion and will be presented in future work.

5. Simulations

We consider the MIMO cognitive radio network where the $(4 \times 4, 3)^2$ MIMO cognitive interference channel is considered, which follows the same manner $(M \times N, d)^K$ for the K-user MIMO cognitive interference channel [35]. The channel is assumed as a flat-fading channel, where each channel element is drawn independently identically distributed (i.i.d) from a complex Gaussian distribution with mean zero and variance 1, and each link has the unit variance of white Gaussian noise. The transmit power is equally allocated to each column of the precoding matrices, that is, $10^{P/10}/d_k$; consequently, the SNR per user is P dB. The algorithms stop once the difference of the objective functions that obtained the two iterations is less than 0.001. Note that, in order to illustrate the effect of the CR interferences on primary transmission, single primary transmission is considered, in which the interferences from its own link are perfectly aligned. Three IA approaches are presented, that is, the interference minimization algorithm subject to the standard constraint, *interference temperature* [25, 36], the proposed rank-constrained interference minimization design, and the developed rank-constrained interference rank minimization approach. For simplicity, we abbreviate the standard approach as IM and the proposed algorithms as *rank-constrained IM* and *rank-constrained IRM*, respectively. Each point is based on 200 Monte Carlo iterations on National Super Computing Center in Guangzhou Tianhe II supercomputer.

5.1. Performance with respect to Fixed Interference Threshold. In this subsection, we present the system performances under the interference temperature and the interference rank constraint and demonstrate the difference between the standard and new metrics, where the thresholds of the interference *metrics* are set equally to $\varepsilon = 1.5$.

The performance of the average sum rate and the achievable multiplexing gain of secondary links is illustrated in Figures 2 and 3, respectively. The proposed rank-constrained IRM approach achieves the highest sum rate due to its highest achievable multiplexing gain, as shown in Figure 3. Meanwhile, compared with the standard IM algorithm, the proposed rank-constrained IM design obtains higher average sum rate. Due to $\|\mathbf{A}\|_F \leq \|\mathbf{A}\|_*$, the nuclear norm surrogate is tighter than the Frobenius norm constraint under the same interference threshold, leading to less interference leaking to the PU-Rx. Consequently, more power would be concentrated on the cognitive transmission, resulting in the improvement on the sum rate of the secondary links. Taking the multiplexing gain as optimization objective, the rank-constrained IM design achieves the highest DoF, followed in order by the proposed rank-constrained IM design and the standard IM design. These two figures clearly demonstrate the key difference between the power minimization approach and the dimension minimization framework (including the two proposed algorithms): the interference minimization focuses on the power minimization with low energy of interference achieved, and the rank minimization designs reduce the dimensions of the subspace spanned by interference matrices. The latter one can provide more interference-free subspace for the indented signal, compared with the former one.

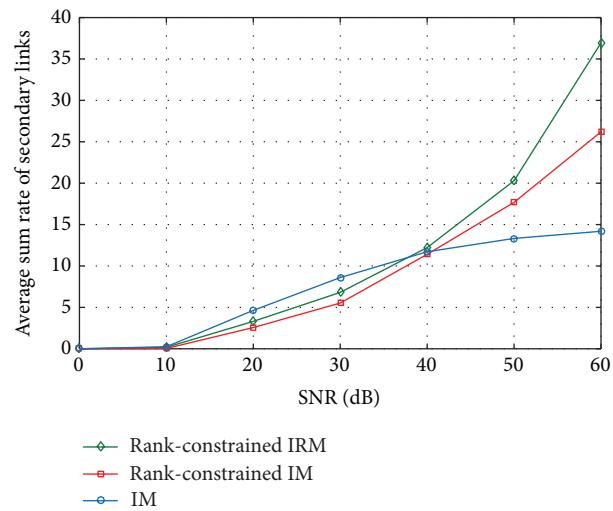

Figure 2: Average sum rate of secondary transmissions versus SNR ($\varepsilon = 0.9$).

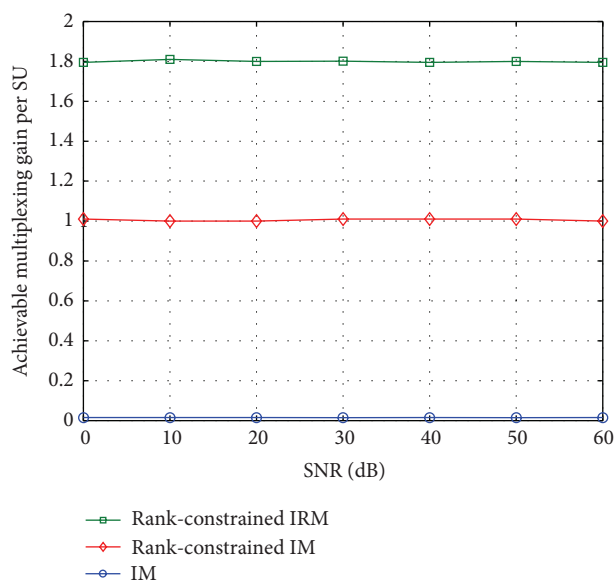

Figure 3: Achievable multiplexing gain of secondary transmissions versus SNR.

To further investigate the effect of the dimension constraint and the power constraint, the performance of the average sum rate and the achievable multiplexing gain of primary link is also presented. In Figure 4, the sum rate of the primary link tends to be a constant, which is caused by CR interferences, even though the rank-constrained IRM approach still obtains the highest sum rate among three algorithms. Figure 5 presents the advantage of the dimension constraint: the CR interferences under standard IM approach contaminate all receiver signal subspaces of the PU, while the interference-free subspace provided by the rank-constrained

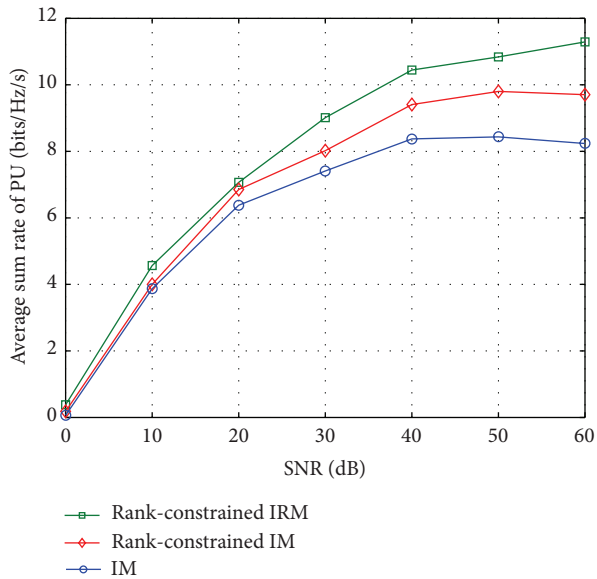

Figure 4: Average sum rate of primary link versus SNR ($\varepsilon = 0.9$).

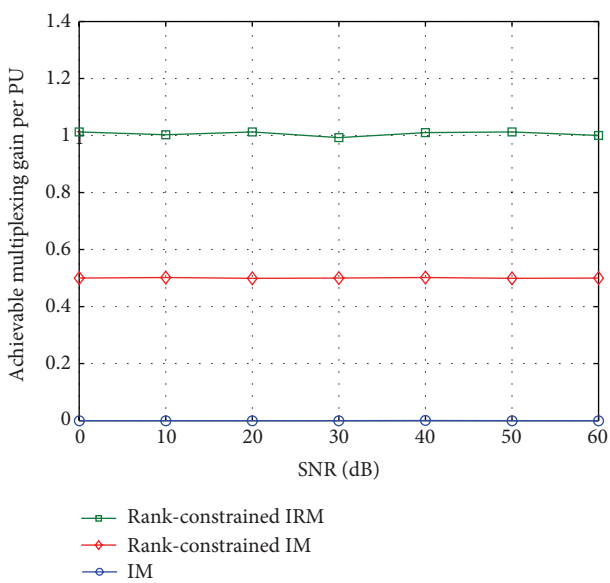

Figure 5: Achievable multiplexing gain of primary link versus SNR.

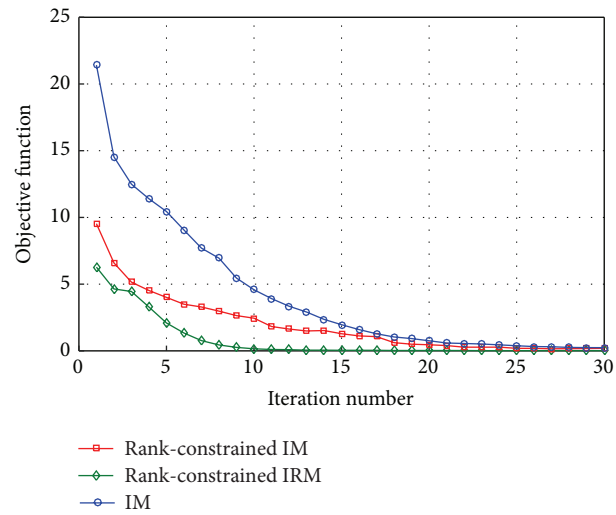

Figure 6: Convergence of the alternating algorithms (SNR = 0 dB).

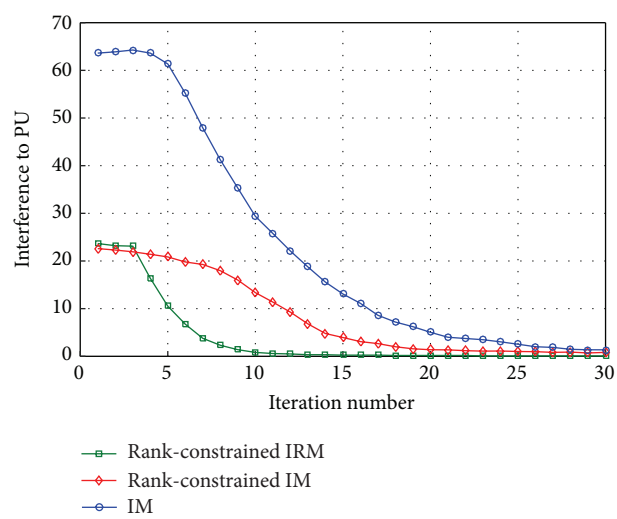

Figure 7: Convergence of the CR interference to PU (SNR = 0 dB).

framework is larger than zero. Both figures show that the dimension constraint could be an effective interference *metric* in the underlay CR network, which can provide higher sum rate and interference-free subspace for the primary transmission.

Furthermore, Figure 6 presents the convergence of the objective function with SNR = 0 dB. As we expected, the objective functions of all three distributed algorithms converge monotonically. The proposed rank-constrained IRM approach has the fastest convergence speed, and the standard IM approach has the slowest one. Figure 7 further investigates the CR interferences to the PU-Rx under the rank-constrained IM, rank-constrained IRM, and IM algorithms. For fair comparison, the power of the CR interferences is taken into account. It is clear that the converged CR interferences under the rank-constrained designs are lower than that under the interference temperature, which on the other hand confirms that the nuclear norm constraint is tighter than the Frobenius norm constraint.

5.2. Performance with respect to Varied Interference Threshold. In this subsection, we investigate the effect of different interference metrics. The SNRs of the cognitive links and primary link are equal to $P = 40$ dB, and the length of the transmitted signals in the primary link is $d_p = d_k = 3$.

Figures 8 and 9 present the performance of the sum rate and the achievable multiplexing gain of the secondary transmission, respectively. In Figure 8, the increased threshold of the interference *metrics* indicates that more power from the secondary links is allowed to leak into the primary transmission, leading to less power transmitting the secondary signals. As a result, the increased threshold degrades the performance

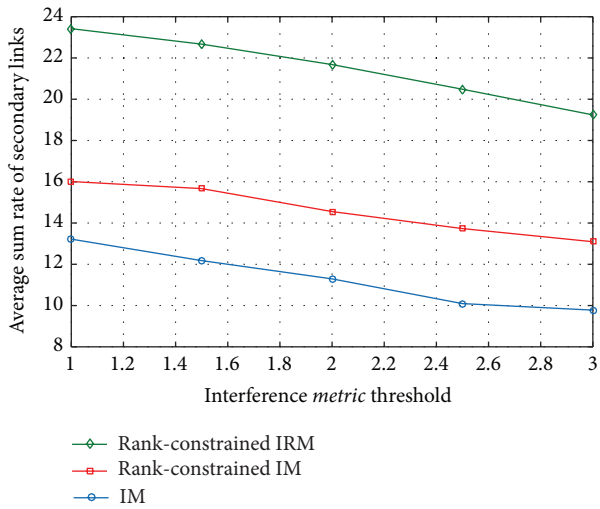

Figure 8: Average sum rate per SU under varied interference threshold.

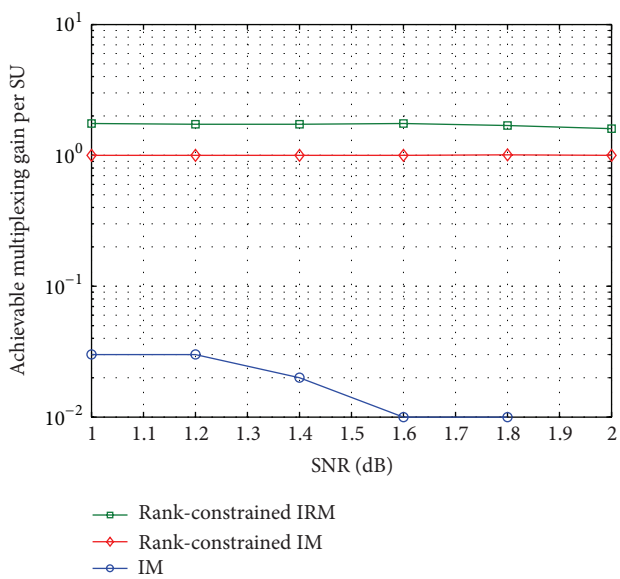

Figure 9: Achievable multiplexing gain per SU under varied interference threshold.

of the sum rate of the secondary links provided by all three algorithms. In terms of the average achievable multiplexing gain of the secondary links, Figure 9 demonstrates the advantage of the dimension maximization of the interference-free receiver subspace. The proposed rank-constrained IRM algorithm provides the best performance among all considered algorithms, followed by the proposed rank-constrained IM algorithm, while the traditional IM algorithm achieves the lowest interference-free subspace. The rank-constraint designs are less sensitive to the varied threshold since the dimensions of the CR interferences are limited to 2 due to $\lceil \varepsilon_i \rceil = 1$ ($i = 1, \ldots, 6$ and $\lfloor x \rfloor$ is the element of x to the nearest integer towards infinity). Compared with the proposed design, the standard IM is very sensitive to the varied threshold, where the achievable DoF becomes zero

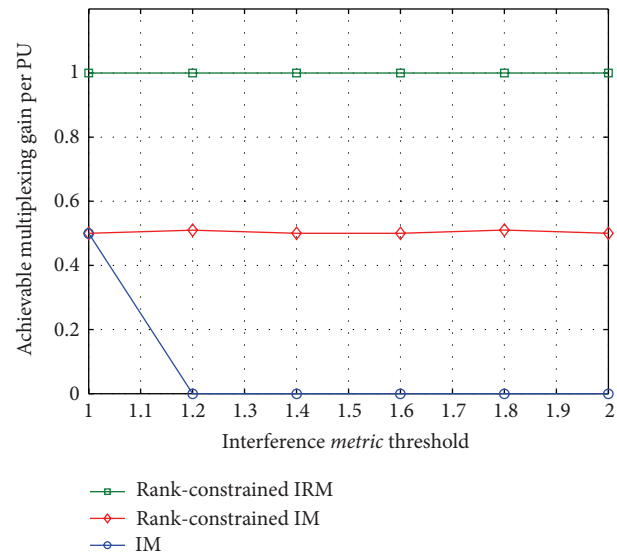

Figure 10: Achievable multiplexing gain per PU under varied interference threshold.

as long as $\varepsilon \geq 1.6$. Both Figures 8 and 9 indicate that the consideration of the dimension optimization is reasonable and effective.

Figure 10 presents the advantage of the developed framework in terms of the average achievable multiplexing gain of the primary link, which provides overall better performance than the IM approach. More specifically, when the threshold increases to 2, the IM designs cannot obtain any multiplexing gain at PU-Rx, while the proposed framework achieves $\mathrm{DoF}_p = 0.5$ (in rank-constrained IM) and $\mathrm{DoF}_p = 1$ (in rank-constrained IRM), respectively. It is because the developed algorithms strive to align the CR interferences into a reduced-dimensional subspace at PU-Rx that only low-dimensional signal subspace would be contaminated by the CR interferences, even if perfect alignment is not achievable at PU-Rx.

In addition, Figure 11 illustrates the iteration number under the varied interference threshold. Interestingly, we find that the rank-constrained IRM algorithm has the lowest computation complexity, and the IM algorithm has the highest complexity, which suggests that the proposed algorithm is practicable.

5.3. Performance with respect to Implicit Advantages. In the subsection, we further explore the implicit advantages of the proposed algorithms in terms of the robustness against imperfect CSI and varied feasibility conditions, shown in Figures 12, 13, and 14, respectively. The imperfect channel state information (CSI) is modeled as $\widehat{\mathbf{H}} = \sqrt{1-\delta}\mathbf{H} + \sqrt{\delta}\mathbf{E}$, where $\delta^2 = 0.15$. Figure 12 shows that the proposed RCRM algorithm has the potential robustness against the imperfections, since the RCRM framework strives to minimize the dimension of the interferences rather than the power.

Moreover, two different feasibility conditions are considered, that is, $(4 \times 4, 2)^3$ and $(4 \times 4, 3)^2$ with single PU ($M_p = N_p = 2$, $d_p = 2$, $P = 1$). When the perfect IA cannot be

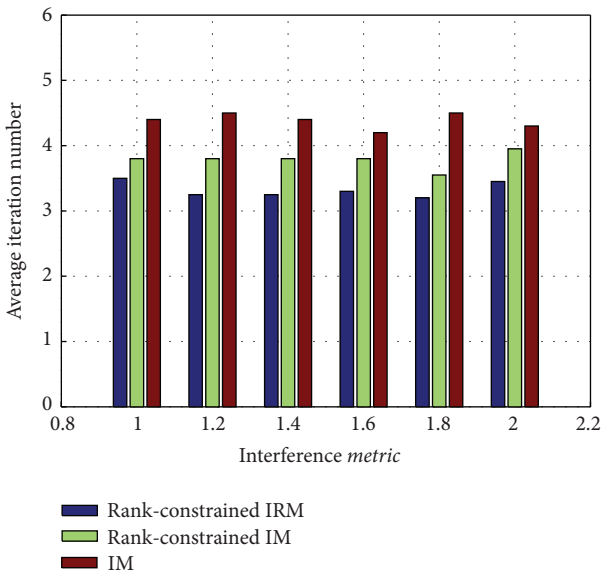

Figure 11: Iteration number under the varied interference threshold.

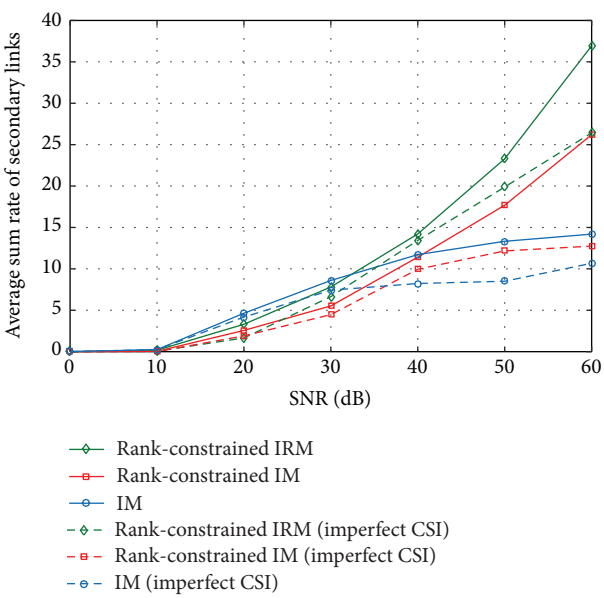

Figure 12: Robustness of the proposed algorithm with respect to average sum rate of secondary transmissions.

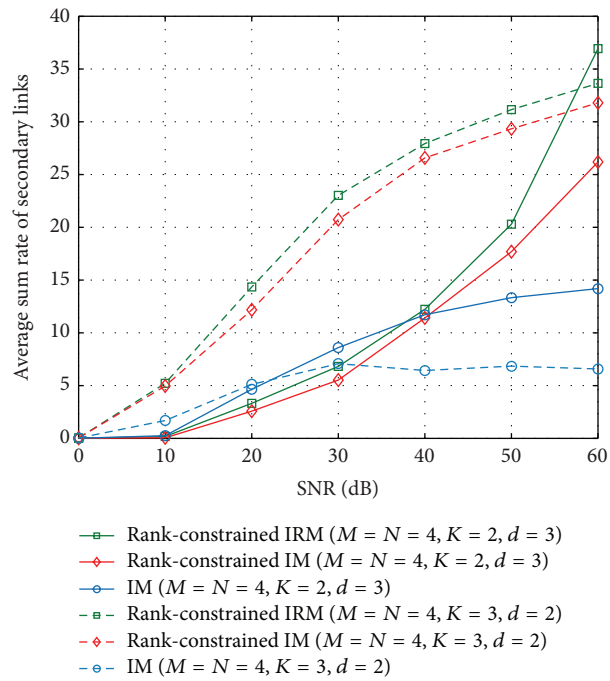

Figure 13: Average sum rate of secondary transmissions with two feasible conditions.

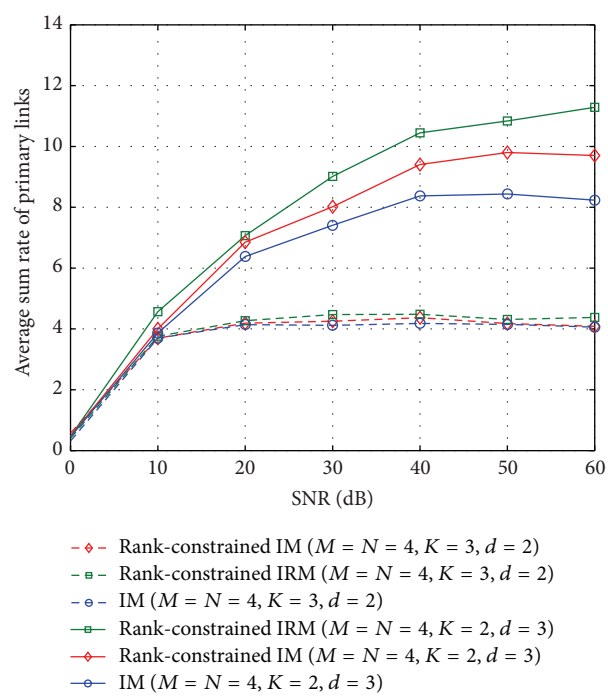

Figure 14: Average sum rate of primary transmissions with two feasible conditions.

achieved, the proposed algorithm still can achieve reasonable performance with no limitation on the number of transmit antennas, receiving antennas, and secondary users and the length of transmit data. In Figures 13 and 14, the higher sum rate of the secondary transmission can be achieved under the configuration of $(4 \times 4, 2)^3$, compared with that under $(4 \times 4, 3)^2$ system in the low and moderate SNR region. However, the curves of the sum rate become flat, which indicates that the interference increases with the increase of SNR, leading to the degradation of the sum rate of primary transmission.

Finally, the scenario that the multiple PUs coexist with multiple SUs is presented in Figure 15. In multiple primary links, we assume that there might exist interferences between multiple primary links by generating the primary receiving beamforming randomly. The sum rate of the secondary links is limited by the multiple CR interference constraints, and its performance of the sum rate is degraded especially in high SNR region. However, the rank-constrained IRM

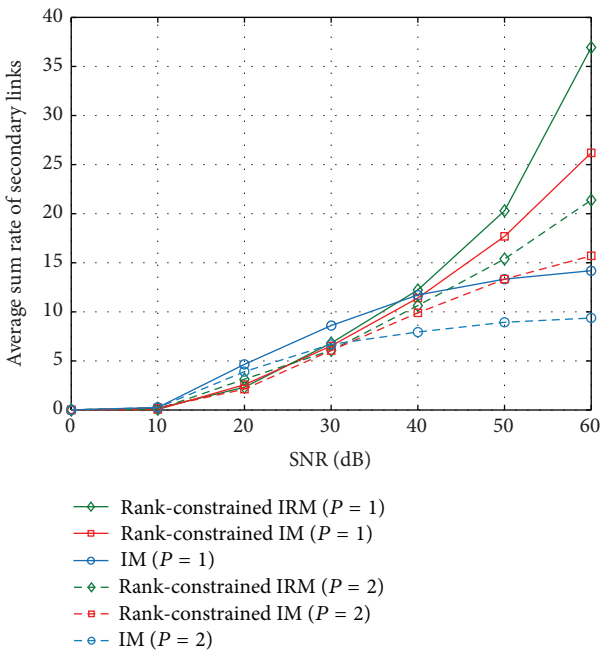

Figure 15: Single PU versus multi-PUs in terms of average sum rate of secondary transmissions.

still achieves the best performance compared with rank-constrained IM and standard IM, due to the rank minimization. The numerical simulation results motivate us to explore the corresponding mathematical background in our future work.

6. Conclusion

In this paper, we developed a rank-constrained beamforming algorithm for MIMO cognitive radio network. Instead of using the *interference temperature*, a rank constraint on CR interferences to the PU-Rxs is proposed, which aligns the CR interferences into a reduced-dimensional subspace. The optimal precoding and receiving beamforming matrices are designed by minimizing the total interferences of the cognitive interference channel subject to the rank constraints on CR interferences and SUs and achieved iteratively via alternating minimization. The rank-constrained design is further improved to minimize the dimension of the interference of the cognitive interference channel. Numerical results show that the proposed algorithm and its development not only improve the achievable average sum rate of the SUs and PU, but also provide more DoF of the interference-free subspace for the primary transmission, under the help of the rank constraint on CR interferences.

Competing Interests

The authors declare that there is no conflict of interests regarding the publication of this paper.

Acknowledgments

The work of Zujian Wu is supported by the Fundamental Research Funds for the Central Universities (no. 21615316) and Special Program for Applied Research on Super Computation of the NSFC-Guangdong Joint Fund (the second phase). The work of Huiqin Du is supported by the Fundamental Research Funds for the Central Universities and National Natural Science Foundation of China (no. 61401178).

References

[1] V. R. Cadambe and S. A. Jafar, "Interference alignment and spatial degrees of freedom of the K-user interference channel," in *Proceedings of the IEEE International Conference on Communications (ICC '08)*, pp. 971–975, May 2008.

[2] S. W. Peters and R. W. Heath Jr., "Interference alignment via alternating minimization," in *Proceedings of the IEEE International Conference on Acoustics, Speech, and Signal Processing (ICASSP '09)*, pp. 2445–2448, April 2009.

[3] K. R. Kumar and F. Xue, "An iterative algorithm for joint signal and Interference Alignment," in *Proceedings of the IEEE International Symposium on Information Theory (ISIT '10)*, pp. 2293–2297, Austin, Tex, USA, June 2010.

[4] B. Nosrat-Makouei, J. G. Andrews, and R. W. Heath Jr., "A simple SINR characterization for linear interference alignment over uncertain MIMO channels," in *Proceedings of the IEEE International Symposium on Information Theory (ISIT '10)*, pp. 2288–2292, Austin, Tex, USA, June 2010.

[5] E. Chiu, V. K. N. Lau, H. Huang, T. Wu, and S. Liu, "Robust transceiver design for K-pairs quasi-static MIMO interference channels via semi-definite relaxation," *IEEE Transactions on Wireless Communications*, vol. 9, no. 12, pp. 3762–3769, 2010.

[6] K. Gomadam, V. R. Cadambe, and S. A. Jafar, "Approaching the capacity of wireless networks through distributed interference alignment," in *Proceedings of the IEEE Global Telecommunications Conference (GLOBECOM '08)*, pp. 4260–4265, New Orleans, La, USA, December 2008.

[7] H. Sung, S.-H. Park, K.-J. Lee, and I. Lee, "Linear precoder designs for K-user interference channels," *IEEE Transactions on Wireless Communications*, vol. 9, no. 1, pp. 291–301, 2010.

[8] H. Huang, V. K. Lau, Y. Du, and S. Liu, "Robust lattice alignment for K-user MIMO interference channels with imperfect channel knowledge," *IEEE Transactions on Signal Processing*, vol. 59, no. 7, pp. 3315–3325, 2011.

[9] H. Yu and Y. Sung, "Least squares approach to joint beam design for interference alignment in multiuser multi-input multi-output inferference channels," *IEEE Transactions on Signal Processing*, vol. 58, no. 9, pp. 4960–4966, 2010.

[10] H. Shen, B. Li, M. Tao, and X. Wang, "MSE-based transceiver designs for the MIMO interference channel," *IEEE Transactions on Wireless Communications*, vol. 9, no. 11, pp. 3480–3489, 2010.

[11] M. Guillaud and D. Gesbert, "Interference alignment in the partially connected K-user MIMO interference channel," in *Proceedings of the 19th European Signal Processing Conference (EUSIPCO '11)*, pp. 1095–1099, Barcelona, Spain, September 2011.

[12] M. Guillaud and D. Gesbert, "Interference alignment in partially connected interfering multiple-access and broadcast channels," in *Proceedings of the IEEE Global Telecommunications*

Conference (GLOBECOM '11), pp. 1–5, IEEE, Houston, Tex, USA, December 2011.

[13] G. Sridharan and W. Yu, "Linear beamformer design for interference alignment via rank minimization," *IEEE Transactions on Signal Processing*, vol. 63, no. 22, pp. 5910–5923, 2015.

[14] F. Negro, S. P. Shenoy, D. T. M. Slock, and I. Ghauri, "Interference alignment limits for K-user frequency-flat MIMO interference channels," in *Proceedings of the 17th European Signal Processing Conference (EUSIPCO '09)*, pp. 2445–2449, Glasgow, Scotland, August 2009.

[15] H. Zhou and T. Ratnarajah, "A novel interference draining scheme for cognitive radio based on interference alignment," in *Proceedings of the IEEE Symposium on New Frontiers in Dynamic Spectrum (DySPAN '10)*, pp. 6–9, April 2010.

[16] J.-M. Wu, T.-F. Yang, and H.-J. Chou, "MIMO active interference alignment for underlay cognitive radio," in *Proceedings of the IEEE International Conference on Communications Workshops (ICC '10)*, pp. 1–5, Cape Town, South Africa, May 2010.

[17] X. Li, N. Zhao, Y. Sun, and F. R. Yu, "Interference alignment based on antenna selection with imperfect channel state information in cognitive radio networks," *IEEE Transactions on Vehicular Technology*, 2015.

[18] L. Sboui, H. Ghazzai, Z. Rezki, and M. S. Alouini, "On achievable rate of two-way relaying cognitive radio with space alignment," in *Proceedings of the IEEE International Conference on Communications (ICC '15)*, pp. 7628–7632, June 2015.

[19] A. Alizadeh, H. R. Bahrami, M. Maleki, and S. Sastry, "Spatial sensing and cognitive radio communication in the presence of a K-user interference primary network," *IEEE Journal on Selected Areas in Communications*, vol. 33, no. 5, pp. 741–754, 2015.

[20] Z. Cheng, N. Devroye, and T. Liu, "The degrees of freedom of full-duplex bidirectional interference networks with and without a MIMO relay," *IEEE Transactions on Wireless Communications*, vol. 15, no. 4, pp. 2912–2924, 2016.

[21] H. Zeng, Y. Shi, Y. T. Hou, W. Lou, S. Kompella, and S. F. Midkiff, "An analytical model for interference alignment in Multi-Hop MIMO networks," *IEEE Transactions on Mobile Computing*, vol. 15, no. 1, pp. 17–31, 2016.

[22] N. Zhao, F. R. Yu, and V. C. M. Leung, "Opportunistic communications in interference alignment networks with wireless power transfer," *IEEE Wireless Communications*, vol. 22, no. 1, pp. 88–95, 2015.

[23] M. Amir, A. El-Keyi, and M. Nafie, "Constrained interference alignment and the spatial degrees of freedom of mimo cognitive networks," *IEEE Transactions on Information Theory*, vol. 57, no. 5, pp. 2994–3004, 2011.

[24] P.-J. Chung, H. Du, and J. Gondzio, "A probabilistic constraint approach for robust transmit beamforming with imperfect channel information," *IEEE Transactions on Signal Processing*, vol. 59, no. 6, pp. 2773–2782, 2011.

[25] S. Ma, H. Du, T. Ratnarajah, and L. Dong, "Robust joint signal and interference alignment in cognitive radio networks with ellipsoidal channel state information uncertainties," *IET Communications*, vol. 7, no. 13, pp. 1360–1366, 2013.

[26] W. Guo, W. Xu, J. Lin, and L. Fu, "Adaptive eigenmodes beamforming and interference alignment in underlay and overlay cognitive networks," in *Proceedings of the IEEE 26th Annual International Symposium on Personal, Indoor, and Mobile Radio Communications (PIMRC '15)*, pp. 798–802, Hong Kong, August 2015.

[27] J. Lee, H. Wang, J. G. Andrews, and D. Hong, "Outage probability of cognitive relay networks with interference constraints," *IEEE Transactions on Wireless Communications*, vol. 10, no. 2, pp. 390–395, 2011.

[28] H. Du, T. Ratnarajah, M. Sellathurai, and C. B. Papadias, "Reweighted nuclear norm approach for interference alignment," *IEEE Transactions on Communications*, vol. 61, no. 9, pp. 3754–3765, 2013.

[29] D. S. Papailiopoulos and A. G. Dimakis, "Interference alignment as a rank constrained rank minimization," *IEEE Transactions on Signal Processing*, vol. 60, no. 8, pp. 4278–4288, 2012.

[30] E. J. Candes, M. B. Wakin, and S. P. Boyd, "Enhancing sparsity by reweighted l1 minimization," *The Journal of Fourier Analysis and Applications*, vol. 14, no. 5-6, pp. 877–905, 2008.

[31] M. Fazel, *Matrix rank minimization with applications [Ph.D. thesis]*, Stanford University, Stanford, Calif, USA, 2002.

[32] M. Grant and S. Boyd, "Matlab software for disciplined convex programming (web page and software)," http://arxiv.org/pdf/0909.4017.

[33] R. A. Horn and C. R. Johnson, *Matrix Analysis*, Cambridge Univeristy Pres, Cambridge, UK, 1985.

[34] S. Boyd and L. Vandenberghe, *Convex Optimization*, Cambridge University Press, Cambridge, UK, 2004.

[35] C. M. Yetis, T. Gou, S. A. Jafar, and A. H. Kayran, "Feasibility conditions for interference alignment," in *Proceedings of the IEEE Global Telecommunications Conference (GLOBECOM '09)*, pp. 1–6, Honolulu, Hawaii, USA, December 2009.

[36] H. Du, T. Ratnarajah, H. Zhou, and Y. C. Liang, "Interference alignment for peer-to-peer underlay MIMO cognitive radio network," in *Proceedings of the 45th Asilomar Conference on Signals, Systems and Computers (ASILOMAR '11)*, pp. 349–353, Pacific Grove, Calif, USA, November 2011.